

Time resolved laser spectroscopy for the *in situ* characterization of methacrylate monomer flow within Spruce

Emma-Rose Janeček · Zarah
Walsh-Korb · Ilaria Bargigia · Andrea
Farina · Michael Ramage · Cosimo
D'Andrea · Austin Nevin · Antonio
Pifferi · Oren A. Scherman*

Received: date / Accepted: date

Abstract Time resolved diffuse optical spectroscopy (TRS) was investigated as a non-destructive method to characterize the post-impregnation distribution of methacrylate monomer within spruce (*Picea abies*). TRS was also used to monitor *in situ* the flow of methacrylate monomers within spruce during impregnation with both spacial and temporal resolution. This *in situ* data was then compared to fluid flow models developed by Darcy and Bramhall demonstrating that neither of these models were able to describe accurately the experimental results, highlighting the need for development of new models. Non-destructive characterization by TRS did not require staining of the monomer treatment solution, multivariate analysis or complex sample pre-treatment thus highlighting the facile applicability of this technique.

Keywords Flow · Impregnation · In situ characterization · Monomer · NIRS · Polymer · Spruce · TRS

Oren A. Scherman*, Emma-Rose Janeček and Zarah Walsh-Korb
Melville Laboratory for Polymer Synthesis, Department of Chemistry, University of Cambridge, United Kingdom
E-mail: oas23@cam.ac.uk

Ilaria Bargigia and Cosimo D'Andrea
Politecnico di Milano, Milano, Italy and Center for Nano Science and Technology@PoliMi,
Istituto Italiano di Tecnologia, Via Giovanni Pascoli 70/3, I-20133, Milano, Italy

Antonio Pifferi
Politecnico di Milano, Milano, Italy

Andrea Farina and Austin Nevin
Consiglio Nazionale delle Ricerche, Istituto di Fotonica e Nanotecnologie, Milano, Italy

Michael Ramage
Department of Architecture, University of Cambridge, United Kingdom

1 Introduction

Flow and sorption within wood are non-trivial processes as evidenced by numerous investigations spanning more than four decades [Devi et al., 2004, Siau, 1984, Bramhall, 1971, Bratasz et al., 2012, Gething et al., 2013, Ahmed et al., 2013, Zhang et al., 2014, Fackler and Thygesen, 2013]. Most of these studies have focused on the sorption of moisture by wood, which has implications for living plants [Tyree and Ewers, 1991] and for timber as a construction material [Bratasz et al., 2012, Xie et al., 2011, Telkki et al., 2013]. Although the majority of studies focus on moisture movement during wetting or drying [Eitelberger et al., 2011, Hill et al., 2010], there have also been investigations into water and solute migration within saturated wood for biorefining purposes [Jacobson et al., 2006]. The movement of supercritical CO₂ within wood is an area that has also recently gained interest as supercritical CO₂ has the ability to act as an environmentally-benign carrier for wood preservatives [Gething et al., 2013, Acda et al., 2001, Muin and Tsunoda, 2004]. With the exception of supercritical CO₂, however, few recent studies exist investigating the *flow* of non-aqueous solutions through wood. Non-aqueous flow has implications for the durability of preservative treated timber. Herein the movement of monomer specifically is of interest. Investigation of the final distribution (topochemistry) of non-aqueous treatments within wood are well known [Mahnert et al., 2013], as are studies into wettability and sorption with non-aqueous media [Moghadam et al., 2014], yet the kinetics and flow processes have not typically been characterized.

Changes in liquid viscosity, surface tension and ability to wet the solid surface have a dramatic effect on the flow behavior within a material, e.g. the rise of fluid within a capillary [Reed and Wilson, 1993, Zhang et al., 2007]. The results gained from the study of moisture within wood cannot be directly applied to monomer movement through wood as many of the physical properties of the liquid have changed. New methods to monitor the movement of non-aqueous solutions are, thus, required.

The treatment of wood with preservatives has long been carried out to extend the in-service life-time of a timber section. Although, some species of wood are regarded as durable and resistant to biological or environmental degradation, other species of wood such as the spruce investigated here are more susceptible to attack [Moore, 2011]. Other treatments have also been carried out in order to increase the dimensional stability or hardness of the wood under investigation. Preservatives which have in the past been utilized extensively include pentachlorophenol and copper chrome arsenate (CCA) [Schultz et al., 2008]. Chemical modification of the wood itself through acetylation or furfurylation and monomer treatment have also been carried out [Jebrane and Sebe, 2008, Chang and Chang, 2003, Evans et al., 2000, Hill et al., 2005, Goldstein and Dreher, 1960, Zhang et al., 2006, Ajjji, 2006]. Some of these treatments rely on aqueous or gaseous transport through wood but others depend on non-aqueous flow processes.

In order to measure the flow of a liquid treatment through wood *in situ*, non-destructive methods are essential so that a single area can be measured repeatedly over time. Non-destructive wood characterization methods such as gamma- or X-ray tomography [Steppe et al., 2004], thermography, as well as microwave, ultrasonic and NMR spectroscopy [Bucur, 2003] are powerful tools for mapping changes in density and, hence, anatomical characteristics within wood [Lindgren et al., 1992]. NMR spectroscopy has even been used in the investigation of the pathways of moisture drainage from softwoods [Almeida et al., 2008]. Other than NMR, however, many non-destructive characterization techniques are unable to chemically identify the treatment material but rather detect changes in the dielectric or density profile of the wood [Bucur, 2003]. Additionally, the detection of treatment solutions may require staining to improve contrast, particularly with X-ray tomography. Moreover, the high energy nature of X-ray and gamma-ray treatment render them unsuitable probes for *in situ* characterization of the monomer movement investigated here as they can initiate polymerization.

Near infrared spectroscopy (NIRS) allows for fast, non-destructive, cost-effective materials characterization with minimal sample preparation [Chen et al., 2010, Foley et al., 1998]. For these reasons NIRS is a favored analytical technique within many industries including agriculture [Morra et al., 1991], food [Cen and He, 2007], textiles [Barton II et al., 2002] and biomedicine [Maki et al., 1995, Durduran et al., 2010]. The use of the so-called therapeutic, or optical, window of wavelengths in the range of 600 - 1300 nm are found to be non-destructive for biological tissue and allows for a depth penetration in some cases of as much as 20-70 mm [Villringer and Chance, 1997]. NIRS has also been applied to the characterization of wood and pulps [Tsuchikawa and Schwanninger, 2013], and more specifically, the analysis of transgenic trees [Yamada et al., 2006], the assessment of lignin in maritime pine [Alves et al., 2006] and quantification of linseed oil uptake [Eriksson et al., 2011, Geladi et al., 2014]. Lande et al. (2010) also used NIRS correlated to thermogravimetric analysis to determine treatment levels in furfuryl treated Scots pine wood flour, but the distribution of polymer through the treated samples was not characterized.

Time-resolved diffuse optical spectroscopy (TRS) using NIR lasers is a sophisticated NIRS technique providing spectra of a sample's absorption and scattering, thus allowing for quantification of different chemical components within the material [Patterson et al., 1989, Cubeddu et al., 1999]. TRS allows for more detailed non-destructive characterization, without the need for multivariate analysis, and has been applied as an oxygen monitor in human tissues [Suzuki et al., 1999] and also for characterization of fruits [Nicolai et al., 2008, Cubeddu et al., 2001]. TRS has previously been used in the characterization of water within wood [D'Andrea et al., 2009] and has been shown to also quantitatively detect monomer [Farina et al., 2014]. Here TRS is applied to the characterization of monomer distribution and *flow* within wood, exploring the utility of this technique for the *in situ* characterization of timber during modification.

2 Materials and methods

All chemicals were purchased from Sigma-Aldrich Ltd (Dorset, United Kingdom) or Acros Organics (Thermo Fisher Scientific, Geel, Belgium) and used as received. Spruce, *Picea abies*, was purchased from Ridgeons Ltd (Cambridge, United Kingdom) and supplied by VIDA (Alvesta, Sweden). Relative humidity (RH) was measured by means of a Lascar EL-USB-2-LCD +, RH/temperature data logger.

All spruce samples were cut from 2 m lengths of 38 mm x 89 mm (2" x 4") taken from the same pallet of kiln-dried wood. The selected 2 m lumber was largely defect free, the grain roughly parallel to the axial direction and the grain spacing homogeneous. The 10 x 10 x 100 mm sample size was cut by hand from 200 mm lengths, which had been sectioned using a bench saw. Other than kiln-drying by the supplier, samples were not dried further prior to impregnation but rather allowed to reach the ambient moisture content in the lab ($35.8 \pm 5\%$ RH, measured over 50 days).

2.1 Sample impregnation

The volume of monomer mixture (Mix) used during sample treatment varied depending on the vessel size required. The composition of Mix was constant with methyl methacrylate (MMA), glycidyl methacrylate (GMA) and ethylene glycol dimethacrylate (EDMA) in a ratio of MMA:GMA:EDMA (45:45:10, wt.%) and the general procedure for its preparation is as follows.

A vessel was charged with azobis(4-cyanovaleric acid) (0.10 g, 0.41 mmol), MMA (9.6 ml, 9.0 g, 90 mmol), GMA (8.4 ml, 8.8 g, 62 mmol), EDMA (1.9 ml, 2.0 g, 10 mmol) and agitated until complete dissolution had occurred. A background TRS data set was collected for the dry wood, then Mix was added to the wood sample and vacuum applied for 1 h. After 1 h the vacuum was released and the sample allowed to soak in Mix for a further 2 h at atmospheric pressure. During the treatment process measurements by TRS were carried out at positions along half the length of the impregnated sample.

When dye was used to color the Mix solution sample impregnation was carried out according to the general method with the exception that 2 mg of rhodamine B dye was added to Mix prior to sample impregnation.

2.2 Time-Resolved diffuse optical Spectroscopy (TRS)

TRS applied here has been described by [Bassi et al., 2007]. The laser source (Fianium, United Kingdom) was a supercontinuum fiber laser emitting pulsed radiation in the range of 450 - 1750 nm, specifically suitable for a portable rack system. The pulses were supplied at a repetition rate of 63 MHz with an approximate duration of tens of picoseconds. The laser beam was first expanded with a beam-expander (Thorlabs, Germany) and then the white light

was dispersed by means of a Pellin-Broca prism. Thus, the selected wavelength was focused onto an adjustable slit in order to achieve better control over the spectral bandwidth. The light was then coupled to an optical fiber and injected into the sample. The power at the sample was in the order of a few milliwatts per injection wavelength. The diffused light re-emitted from the sample was collected by means of another optical fiber and delivered to a photo-multiplier tube, PMT (Hamamatsu, Japan). The PMT is sensitive to the single-photon level and works in the spectral region 950 - 1400 nm with a quantum efficiency of about 2 % over the whole working range. A time-correlated single photon counting board was employed as timing electronics. Data acquisition is fully automated. Importantly the system used was an entirely portable instrument, designed with the specific purpose of performing measurements in the field.

Automation of the sample set-up was achieved by mounting the sample in a metal plate which was then attached to a stepper motor. The metal plate allowed the sample to be mounted rigidly in contact with the input and output optical fibers yet still moved horizontally allowing measurements to be taken at different positions along the samples' length. A schematic of the experimental set-up is shown in Figure 1. The wood section was held in place within the metal plate by six springs to minimize the surface coverage.

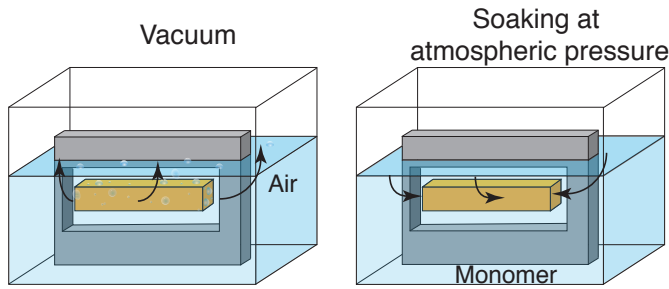


Fig. 1 Schematic of the experimental setup with a graphical representation of air and monomer flow under the different impregnation steps

Fitting of the TRS data was then carried out in accordance with the method as described by [Farina et al., 2014]. Each time-resolved curve collected was fitted according to a time-resolved analytical diffusion equation with a refractive index of 1.17 [Juttula and Makynen, 2012] in order to obtain an absorption spectrum expressed in cm^{-1} . The absorption spectrum was then fitted to a percentage concentration of natural wood, water and Mix using the Lambert-Beer law:

$$\mu_a(\lambda) = \sum c_i \epsilon_i(\lambda) \quad (1)$$

where $\mu_a(\lambda)$ is the absorption spectrum, c_i are the component concentrations, and $\epsilon_i(\lambda)$ represents the reference spectrum of the i th component. It was assumed during this fitting that Mix and water alone fill the air space

in the wood during impregnation and, therefore, the sum of the percentage variation in air, Mix and water is zero. This allows for an iterative update of the refractive index of the sample at each reading as air was replaced by Mix during the impregnation and, hence, for the quantification of Mix. The percentage concentrations of Mix, water and natural wood in each measurement were then converted in to g cm^{-3} based on the density of each component in their pure state.

3 Results and discussion

[Farina et al., 2014] demonstrated that TRS can be used to non-destructively quantify monomer within a sample of treated spruce. Here the technique was extended to characterize the distribution of monomer at specific positions along the longitudinal length of Mix-treated samples, Figure 2. TRS measurements were taken at 10 mm intervals along the longitudinal length of 8 different samples post-impregnation. The position 10 mm from the longitudinal end of the sample being position 1 and subsequent positions numbered accordingly. A step size of 10 mm was chosen as the lateral penetration sampled by the laser was found to be on the order of 5 mm within this sample type. Boundary effects were detected when measurements were taken closer than 5 mm to the edge of the sample.

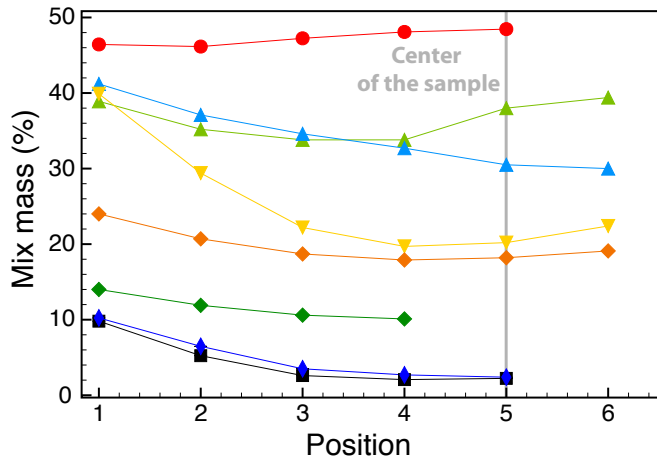


Fig. 2 Mix mass concentration profile as quantified by TRS measured over 8 different 100 mm samples. Each color represents data collected from a different sample. Data sets with different colors but the same symbol indicates end matched samples. Position multiplied by 10 is the longitudinal distance in millimeters from the closest end of the sample

All samples in Figure 2, with the exception of the data shown in (red) circles, display a similar profile with higher Mix concentration at the end of

the sample relative to the center, a distribution typical for wood impregnation [Kolavali and Theliander, 2013, Ahmed et al., 2013]. There was a significant variation in measured Mix mass percentage between the different samples investigated. This variation in Mix mass percentage measured relative to the total mass of the sample is thought to be indicative of differences in permeability and microstructure between samples, a result of natural variation. The different distribution pattern of the data in (red) circles, Figure 2, compared with other samples is thought to be an indication of significantly increased permeability in this specific sample, perhaps arising from micro-cracks invisible by eye. Alternatively, variation in the angle of the grain relative to the samples' longitudinal axis or changes in the sapwood content of the sample are possible explanations for the variation in Mix mass distribution. The scattering data of the sample shown in (red) circles did display a different scattering coefficient when compared to the other samples tested, supporting the suggestion that changes in grain orientation could be the cause.

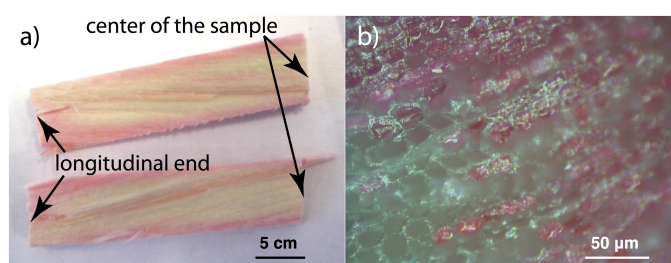


Fig. 3 Images of dye within monomer-impregnated spruce, post-polymerization. a) Optical image of the internal surface of one longitudinal half of a treated sample. b) Optical microscopy image of polymer filled and unfilled cells

Polymer distribution was then investigated visually and microscopically to confirm correlation with Mix mass distribution as determined by TRS. Dye molecules were doped into Mix and the arrangement, post-polymerization, of dyed polymer within the wood visualized on the macroscopic level, Figure 3a). It was evident that at the left-hand end of the sample, Figure 3a), which was in direct contact with Mix, there was more polymer than towards the center. Figure 3b) illustrates the co-localization of polymer and dye as the cells with polymer-filled lumen are also dyed pink and there was no evidence of pink areas without the presence of polymer. Scanning electron micrographs (SEM) taken from sections at the end and middle of the treated wood also indicated higher polymer content at the end of the sample where many lumen were filled compared to the center of the sample where empty cell lumen predominate. In both cases destructive characterization of polymer distribution was in agreement with the monomer distribution prior to polymerization as determined by TRS, demonstrating the suitability of this technique for non-destructive assessment of Mix distribution. It also suggests that no significant movement of Mix occurred at the elevated temperatures during polymerization as the dis-

tribution of polymer resembles that of the monomer. The limited mass change before and after polymerization is in agreement with this conclusion.

TRS can be carried out at atmospheric pressure, under vacuum and when submerged as the optical fibers used were resistant to variations in pressure and chemical attack. This allowed for *in situ* TRS measurements of Mix concentration within the spruce samples during impregnation. *In situ* monitoring enabled a profile of Mix transport to be determined through the wood with both spatial and temporal resolution.

In order to minimize microstructure differences, and allow for meaningful comparison of rates of increase in Mix mass percentage measured relative to the total mass of the sample at different positions, a single sample was measured at four different position during the impregnation process. There was no significant increase in Mix mass percentage measure relative to the total mass of the sample within the wood during the applied vacuum, first 55-65 min, Figure 4. This indicates that application of vacuum resulted in the removal of air from the wood and not Mix uptake, as illustrated schematically in Figure 1, left. Once vacuum was removed the Mix mass percentage within the wood rapidly increased at all positions, Figure 4, indicating Mix infiltration of the wood.

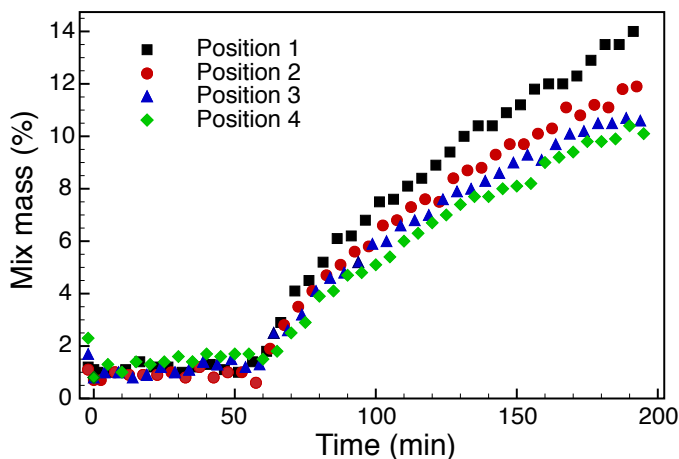


Fig. 4 Percentage of Mix relative to the total mass of the treated sample, per cm^3 , calculated from spectra taken at a specific positions along the length of one spruce sample during treatment and monitored over time. Time = 0 min, monomer added to the sample and vacuum applied. Time = 60 min (± 5 min), vacuum released and samples allowed to soak in Mix at atmospheric pressure

Figure 4 shows Mix concentration measured at positions 1, 2, 3 and 4 along a single spruce sample measured during impregnation treatment. The rate of Mix mass percentage measured relative to the total mass of the sample increased fastest at position 1 and slowest at position 4, which is consistent with the final Mix distribution determined by TRS, Figure 2. Initial results, Figure

S1, measured at different positions on different samples suggest that variation in microstructure between different wood samples had greater influence on the rate at which Mix was able to flow through the wood than the position at which measurements were taken. Observation of the positional dependance on the rate of Mix uptake was, therefore, only possible when comparing different positions along a single sample.

Under an applied external force Darcy's law is commonly used to describe flow through porous media. Examination of flow by Darcy's law has found application in describing extraction of petrochemicals from geological formation, water movement through bedrock, and chromatography, though there are well known regimes where experiments deviate from the model [Hlushkou and Tallarek, 2006]. It has also been extensively applied to the characterization of various types of flow within wood [Gronli and Melaaen, 2000, Fredeen and Sage, 1999, Perre and Turner, 2001]. Darcy's law for liquids in its derivative form can be written as follows [Siau, 1984]:

$$\frac{dV}{dt} = \frac{KA\Delta P}{\eta x} \quad (2)$$

Where $dV = v_a A dx$, K = specific permeability ($\text{m}^3 \text{m}^{-1}$), x = penetration depth (m), η = dynamic viscosity (Pa s), A = cross-sectional area perpendicular to flow (m^2), ΔP = pressure differential (Pa) and v_a = porosity or void volume fraction of wood. Once rearranged:

$$\int_0^x x dx = \frac{K\Delta P}{v_a\eta} \int_0^t dt \quad (3)$$

and the integration performed:

$$x = \sqrt{\frac{2K\Delta Pt}{v_a\eta}} \quad (4)$$

Equation 4 demonstrates that x , the penetration depth of the liquid, should have a \sqrt{t} dependance. The TRS experiments performed did not, however, measure the extent of permeation with time but rather variation in Mix mass percentage at a certain location with time. The plots derived from these experiments are plots of density weighted Mix percentage retention against time. Based on calculations shown by [Siau, 1984] assuming total filling of the voids from the longitudinal end of the sample to the liquid-gas interface:

$$F_{vl} = \frac{2x}{L} \quad (5)$$

Where F_{vl} is the fractional volumetric retention and L is the longitudinal length of the sample. Substituting the equation for x from Darcy's law then gives:

$$F_{vl} = \frac{2}{L} \sqrt{\frac{2K\Delta Pt}{v_a\eta}} \quad (6)$$

According to Equation 6 F_{vl} over the whole sample has a \sqrt{t} dependence. Figure 5 confirms a broadly linear relationship with \sqrt{t} at each position measured. The gradient of the Mix mass percentage *vs.* \sqrt{t} plot, however, varies with the position at which the data was measured. Position 1 has the steepest gradient and position 4 the shallowest, Figure 5. This suggests that Darcy's law does not accurately describe the flow of monomer through the spruce wood investigated as the model cannot account for the position dependence of monomer accumulation. Moreover, the penetration of the sample with Mix is not proportional to \sqrt{t} as predicted by Equation 4, Figure 4, nor does it proceed as a single liquid – gas interface. As shown in Figure 4, Mix is detected by TRS measurements at position 4 after only a short period of time, and Mix continues to accumulate at all positions throughout the duration of the measurement period. This behavior is not in accordance with Darcy's law and suggests that multiple gas-liquid interfaces are moving at different rates through the wood, rather than a single front.

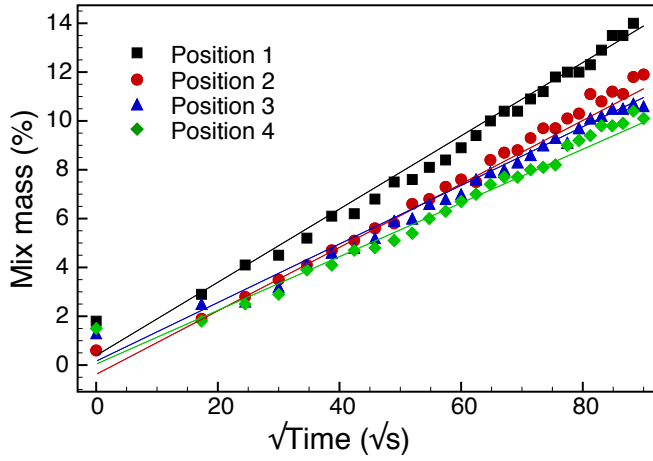


Fig. 5 Plot of Mix mass% *vs.* \sqrt{t} . Solid lines indicate linear best fit, the colors correspond to the four positions

An apparent decreasing sample permeability with increasing length has previously been observed and modelled by [Bramhall, 1971] who found that for some less permeable wood species, such as spruce, axial impregnation was not well described by Darcy's law. In this model it was proposed that the random blockage of tracheids by pit aspiration, insoluble extractives, etc. lead to the exponential decrease in the number of conductive tracheids with increasing penetration depth [Bramhall, 1971]. This behaviour then leads to a decrease in the apparent permeability of the wood with increasing sample length and incomplete filling of voids within the sample.

The assumption of total filling of the voids made during data analysis using Darcy's law was not valid for the samples under consideration, as SEM

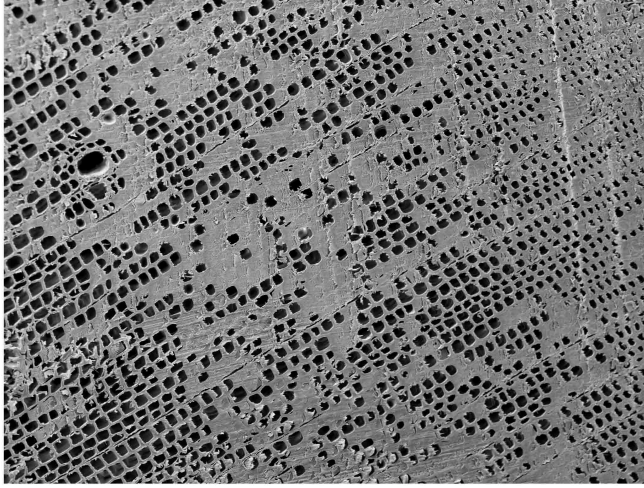


Fig. 6 SEM image of a cross-section of the internal surface of spruce impregnated with Mix and polymerized *in situ*. Empty cell lumen (black) and those filled with polymer (gray) are evident

analysis clearly shows voids within the impregnated and polymerized samples, Figure 6. Mix is thought to shrink upon polymerization and, therefore, could contribute to some of the voids seen in Figure 6, however, this cannot explain the deviation in monomer flow from Darcy's law. Bramhall's model, and specifically incorporation of incomplete filling into the model, was thus investigated. Bramhall's modified version of Darcy's law is given by:

$$\frac{dV}{dt} = \frac{K_0 A e^{-bx} \Delta P}{\eta x} \quad (7)$$

Where K_0 is the permeability at zero length and b is the exponential coefficient describing the decrease in number of conducting fiber tracheids with increasing length. The related fractional volumetric retention accounting for penetration from both ends of the sample as shown by [Siau, 1984] is given by:

$$F_{vl} = \frac{2}{Lb} (1 - e^{-bc\sqrt{t}}) \quad (8)$$

Where c is the combination of constants describing the relationship between x and \sqrt{t} , Equation 4. This indicates that F_{vl} over the whole sample has an exponential dependance on \sqrt{t} rather than the linear dependance predicted by Darcy's law. Summation of Mix mass percentage over all points measured during a certain time period can give an indication of the F_{vl} in the half of the sample measured by TRS. If the sample is assumed to be symmetric, then doubling the sum of Mix mass percentage measured in one half of the sample allows for estimation of the total Mix mass percentage in the whole sample and comparison to Bramhall's model. It must be noted that this method to

estimate the total Mix mass percentage in the whole sample does not account for the Mix uptake in the 5 mm at each end of the sample nor the central 10 mm as these areas were not measured by TRS, however, it is assumed that this does not significantly effect the overall profile of the plot. When plotted against \sqrt{t} the sum of Mix mass percentage, doubled to estimate the mass in the whole sample, shows a relatively linear profile, except for at short times, as seen in Figure 7. This was then fitted according to equations in the form of Bramhall's and Darcy's models.

$$y = mx \quad (9)$$

Equation 9 describes the linear dependance of F_{vl} on \sqrt{t} as predicted by Darcy's law. Bramhall's model in contrast predicts F_{vl} dependance on \sqrt{t} to have the form of Equation 10.

$$y = A(1 - e^{-Bx}) \quad (10)$$

The results shown in Figure 7 demonstrate that the mass increase over the whole sample is better described by Bramhall's model than by Darcy's as there is better agreement between Equation 10 and the experimental data than with the linear fit according to Equation 9. Moreover, the decreasing number of conducting tracheids with increasing sample length as predicted by Bramhall can explain the decreasing rate of monomer accumulation when moving from position 1 to position 4 as the effective permeability at position 4 is decreased compared to position 1.

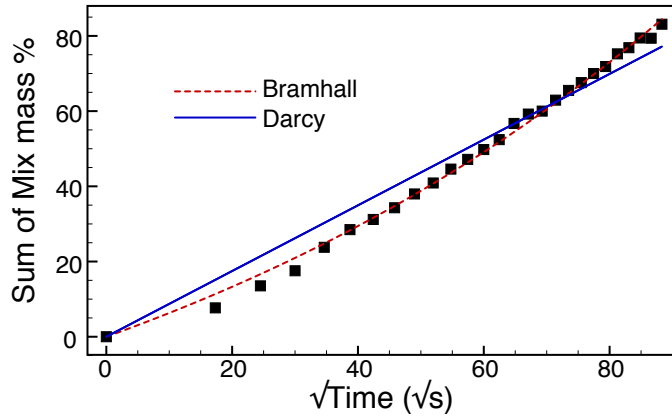


Fig. 7 The sum of Mix percentage over all 4 positions measured doubled to take account of the other half of the sample plotted against the square root of time in seconds. The data has been adjusted to start from monomer percentage = 0. Time = 0, is the removal of vacuum from the sample

Comparing Equation 10 with Equation 8 the constants A and B in Equation 10 should both be positive, however, the fitting shown in Figure 7 arising

from Equation 10, results in small but negative values for A and B . This suggests that b , the exponential coefficient describing the decrease in number of conducting tracheids with increasing length in Equation 8 must also be negative. Bramhall's model, however, relies on a positive value of b . Thus, faster measurements in the time immediately after the vacuum is released and also measurements at much longer time periods would be required to more conclusively determine if the deviation from Darcy's law shown in Figure 7 is real and if Bramhall's model fitted over a longer time period would result in a positive value of b . With the data shown relatively small errors in the first 5 data points after the vacuum was released would have a significant influence on the fitting of the data.

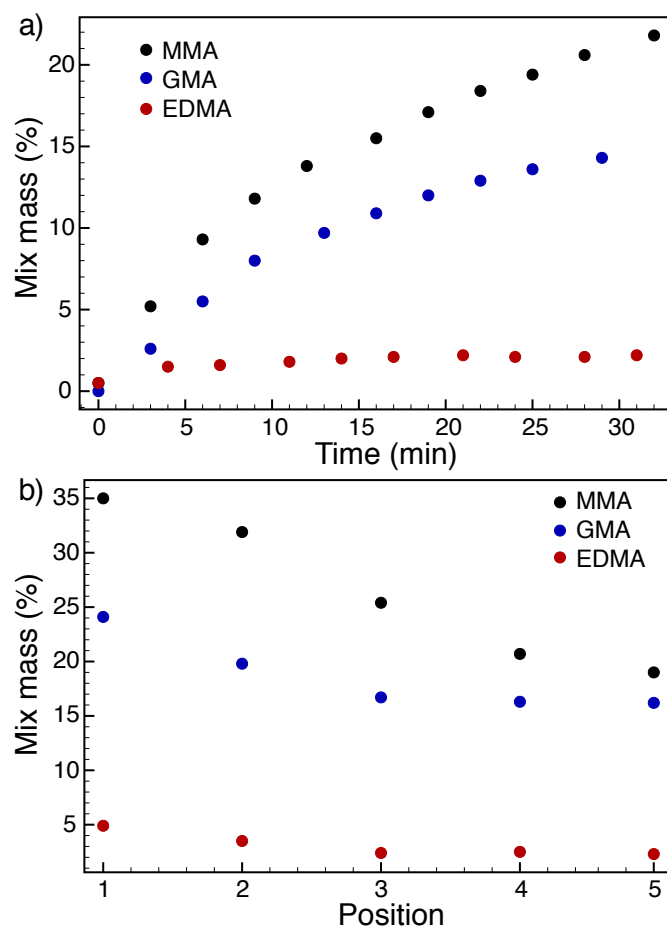


Fig. 8 Percentage of monomer relative to the total mass of the treated sample, per cm^3 calculated from spectra taken from three different sample treated with black) MMA, blue) GMA and red) EDMA. a) at position 3 during the impregnation process and b) at different positions after impregnation

To further examine the utility of the TRS technique for monomer treatment characterization and demonstrate that the technique is not limited to Mix alone. TRS was used to monitor the impregnation of spruce with the individual monomers MMA, GMA and EDMA, Figure 8. Impregnation of porous media is generally viscosity dependant as depicted by Darcy's law and other models of fluid dynamics. The rate of monomer accumulation should also display a viscosity dependance.

MMA and GMA treatments were performed separately on two end-matched samples. The natural permeability of the sections was, therefore, assumed to be comparable. The slower increase in GMA concentration with time when compared to MMA suggests that the more viscous GMA moved more slowly within the wood in accordance with the expected behavior. Additionally, EDMA which has a higher viscosity again, moved even slower. It must be noted that EDMA treatment was carried out on a separate section of spruce, therefore, variation in sample permeability will have an effect. The movement of EDMA was slower than that seen for any of the Mix treated samples, which does suggest that the slower kinetics are viscosity related rather than due to different microstructure. In each case the distribution of monomer through the samples displayed the same profile as the Mix treated samples, Figure 8 b), indicating that although the kinetics are slowed by increasing viscosity, the distribution profile was unaffected.

4 Conclusion

TRS allowed for static, non-destructive, quantitative analysis of monomer distribution within impregnated wood. The distribution profile determined by TRS was consistent with previous literature and destructive characterization of polymer distribution. This indicates great potential for the use of TRS in impregnated wood composite materials as a quantitative method for non-destructive characterization of treatment distribution in the field.

Moreover, TRS was able to demonstrate that the impregnation of even relatively small spruce samples with monomer cannot be accurately described by Darcy's law as it does not describe accurately the local changes in Mix concentration. Bramhall's description of fluid flow within wood was also found to be an inadequate model for the monomer accumulation data as measured by TRS. Although equations in the form of Bramhall's model provided a better fit of the experimental data, the results of the fitting did not lead to physically meaningful results. Additionally, spruce impregnation with monomer of varying viscosity monitored by TRS displayed decreasing monomer flow kinetics with increasing viscosity, again as predicted by fluid mechanics.

Taken together these results demonstrate that TRS is a powerful, non-destructive characterization technique for monomer treated wood. Moreover, TRS allows for post-impregnation and *in situ* measurements of treatment accumulation providing access to data on the kinetics and flow of monomer through wood.

Acknowledgements The authors would like to thank Prof. Paul Linden and Dr. Henry Burrige for useful discussion during the preparation of this manuscript and the EPSRC, ERC Starting investigators grant (ASPiRe, 240629), CUSBO, FP7 Laserlab-europe (n.284464) and the Walters Kundert Trust for financial support.

References

- [Acda et al., 2001] Acda, M. N., Morrell, J. J., and Levien, K. L. (2001). Supercritical fluid impregnation of selected wood species with tebuconazole. *Wood Sci. Technol.*, 35:127–136.
- [Ahmed et al., 2013] Ahmed, S. A., Hansson, L., and Moren, T. (2013). Distribution of preservatives in thermally modified scots pine and norway spruce sapwood. *Wood Sci. Technol.*, 47:499–513.
- [Aji, 2006] Aji, Z. (2006). Preparation of pinewood/polymer/composites using gamma irradiation. *Radiat. Phys. Chem.*, 75:1075–1079.
- [Almeida et al., 2008] Almeida, G., Leclerc, S., and Perre, P. (2008). Nmr imaging of fluid pathways during drainage of softwood in a pressure membrane chamber. *Int. J. Multiphas. Flow.*, 34:312–321.
- [Alves et al., 2006] Alves, A., Schwanninger, M., Pereira, H., and Rodrigues, J. (2006). Calibration of nir to assess lignin composition (h/g ratio) in maritime pine wood using analytical pyrolysis as the reference method. *Holzforschung*, 60:29–31.
- [Barton II et al., 2002] Barton II, F. E., Akin, D. E., Morrison, W. H., Ulrich, A., and Archibald, D. D. (2002). Analysis of fiber content in flax stems by near-infrared spectroscopy. *J. Agric. Food Chem.*, 50:7576–7580.
- [Bassi et al., 2007] Bassi, A., Farina, A., D’Andrea, C., Pifferi, A., Valentini, G., and Cubeddu, R. (2007). Portable, large-bandwidth time-resolved system for diffuse optical spectroscopy. *Opt. Express*, 15:14482–14487.
- [Bramhall, 1971] Bramhall, G. (1971). The validity of darcy’s law in the axial penetration of wood. *Wood Sci. Technol.*, 5:121–134.
- [Bratasz et al., 2012] Bratasz, L., Kozłowska, A., and Kozłowski, R. (2012). Analysis of water adsorption by wood using the guggenheim-anderson-de boer equation. *Eur. J. Wood Prod.*, 70:445–451.
- [Bucur, 2003] Bucur, V. (2003). Techniques for high resolution imaging of wood structure: A review. *Meas. Sci. Technol.*, 14:91–98.
- [Cen and He, 2007] Cen, H. and He, Y. (2007). Theory and application of near infra-red reflectance spectroscopy in determination of food quality. *Trends Food Sci. Tech.*, 18:72–83.
- [Chang and Chang, 2003] Chang, H.-T. and Chang, S.-T. (2003). Improvements in dimensional stability and lightfastness of wood by butyrylation using microwave heating. *J. Wood Sci.*, 49:455–460.
- [Chen et al., 2010] Chen, G., Mei, Y., Tao, W., Zhang, C., Tang, H., Iqbal, J., and Du, Y. (2010). Micro near infrared spectroscopy (micronirs) based on on-line enrichment: Determination of trace copper in water using glycidyl methacrylate-based monolithic material. *Anal. Chim. Acta*, 670:39–43.
- [Cubeddu et al., 2001] Cubeddu, R., D’Andrea, C., Pifferi, A., Taroni, P., Torricelli, A., Valentini, G., Dover, C., Johnson, D., Ruiz-Altisent, M., and Valero, C. (2001). Non-destructive quantification of chemical and physical properties of fruits by time-resolved reflectance spectroscopy in the wavelength range 650-1000 nm. *Appl. Optics*, 40:538–543.
- [Cubeddu et al., 1999] Cubeddu, R., Pifferi, A., Taroni, P., Torricelli, A., and Valentini, G. (1999). Noninvasive absorption and scattering spectroscopy of bulk diffusive media: An application to the optical characterization of the human breast. *Appl. Phys. Lett.*, 74:874.
- [D’Andrea et al., 2009] D’Andrea, C., Nevin, A., Farina, A., Bassi, A., and Cubeddu, R. (2009). Assessment of variations in moisture content of wood using time-resolved diffuse optical spectroscopy. *Appl. Optics*, 48:B87–B93.
- [Devi et al., 2004] Devi, R. R., Maji, T. K., and Banerjee, A. N. (2004). Studies on dimensional stability and thermal properties of rubber wood chemically modified with styrene and glycidyl methacrylate. *J. Appl. Polym. Sci.*, 93:1938–1945.

- [Durduran et al., 2010] Durduran, T., Choe, R., Baker, W. B., and Yodh, A. G. (2010). Diffuse optics for tissue monitoring and tomography. *Rep. Prog. Phys.*, 73:076701.
- [Eitelberger et al., 2011] Eitelberger, J., Svensson, S., and Hofstetter, K. (2011). Theory of transport processes in wood below the fiber saturation point. physical background on the microscale and its macroscopic description. *Holzforschung*, 65:337–342.
- [Eriksson et al., 2011] Eriksson, D., Geladi, P., and Ulvcróna, T. (2011). Near-infrared spectroscopy for the quantification of linseed oil uptake in scots pine (*pinus sylvestris* l.). *Wood Mater. Sci. Eng.*, 6:170–176.
- [Evans et al., 2000] Evans, P. D., Wallis, A. F. A., and Owen, N. L. (2000). Weathering of chemically modified wood surfaces: Natural weathering of scots pine acetylated to different weight gains. *Wood Sci. Technol.*, 34:151–165.
- [Fackler and Thygesen, 2013] Fackler, K. and Thygesen, L. G. (2013). Micro-spectroscopy as applied to the study of wood molecular structure. *Wood Sci. Technol.*, 47:203–222.
- [Farina et al., 2014] Farina, A., Bargigia, I., Janeček, E.-R., Walsh, Z., D’Andrea, C., Nevin, A., Ramage, M., Scherman, O. A., and Pifferi, A. (2014). Nondestructive optical detection of monomer uptake in wood polymer composites. *Optics. Lett.*, 39:228–231.
- [Foley et al., 1998] Foley, W. J., McIlwee, A., Lawler, I., Aragones, L., Woolnough, A. P., and Berding, N. (1998). Ecological application of near infrared reflectance spectroscopy - a tool for rapid, cost-effective prediction of the composition of plant and animal tissues and aspects of animal performance. *Oecologia*, 116:293–305.
- [Fredeen and Sage, 1999] Fredeen, A. L. and Sage, R. F. (1999). Temperature and humidity effects on branchlet gas-exchange in white spruce: an explanation for the increase in transpiration with branchlet temperature. *Trees*, 14:161–168.
- [Geladi et al., 2014] Geladi, P., Eriksson, D., and Ulvcróna, T. (2014). Data analysis of hyperspectral nir image mosaics for the quantification of linseed oil impregnation in scots pine wood. *Wood Sci. Technol.*, 48:467–481.
- [Gething et al., 2013] Gething, B. A., Janowiak, J. J., and Morrell, J. J. (2013). Using computational modeling to enhance the understanding of the flow of supercritical carbon dioxide in wood materials. *J. Supercrit. Fluid.*, 82:27–33.
- [Goldstein and Dreher, 1960] Goldstein, I. S. and Dreher, W. A. (1960). Stable furfuryl alcohol impregnation solutions. *Ind. Eng. Chem.*, 52:57–58.
- [Gronli and Melaaen, 2000] Gronli, M. and Melaaen, M. C. (2000). Mathematical model for wood pyrolysis-comparison of experimental measurements with model predictions. *Energ. Fuel*, 14:791–800.
- [Hill et al., 2005] Hill, C. A. S., Forster, S. C. and Farahani, M. R. M., Hale, M. D. C., Oromdroyd, G. A., and Williams, G. R. (2005). An investigation of cell wall micropore blocking as a possible mechanism for the decay resistance of anhydride modified wood. *Int. Biodeter. Biodegr.*, 55:69–76.
- [Hill et al., 2010] Hill, C. A. S., Norton, A. J., and Newman, G. (2010). The water vapour sorption properties of sitka spruce determined using a dynamic vapour sorption apparatus. *Wood Sci. Technol.*, 44:497–514.
- [Hlushkou and Tallarek, 2006] Hlushkou, D. and Tallarek, U. (2006). Transition from creeping via viscous-inertial to turbulent flow in fixed beds. *J. Chromatogr. A.*, 1126:70–85.
- [Jacobson et al., 2006] Jacobson, A. J., Smith, G. D., Yang, R., and Banerjee, S. (2006). Diffusion of sulfide into southern pine (*pinus taeda* l.) and sweetgum (liquidamber styraciflua l.) particles and chips. *Holzforschung*, 60:498–502.
- [Jebrane and Sebe, 2008] Jebrane, M. and Sebe, G. (2008). A new process for the esterification of wood by reaction with vinyl esters. *Cabohyd. Polym.*, 72:657–663.
- [Juttula and Makynen, 2012] Juttula, H. and Makynen, A. J. (2012). Instrument measurement technology conference, ieee. pages 1–4.
- [Kolavali and Theliander, 2013] Kolavali, R. and Theliander, H. (2013). Determination of the diffusion of monovalent cations into wood under isothermal conditions based on licl impregnation of norway spruce. *Holzforschung*, 67:559–565.
- [Lande et al., 2010] Lande, S., van Riel, S., Hoibo, O. A., and Schneider, M. H. (2010). Development of chemometric models based on near infrared spectroscopy and thermogravimetric analysis for predicting the treatment level of furfurylated scots pine. *Wood Sci. Technol.*, 44:189–203.

- [Lindgren et al., 1992] Lindgren, O., Davis, J., Wells, P., and Shadbolt, P. (1992). Non-destructive wood density distribution measurements using computer tomography. *Holz Roh Werkst.*, 50:295–299.
- [Mahnert et al., 2013] Mahnert, K.-C., Adamopoulos, S., Koch, G., and Militz, H. (2013). Topochemistry of heat-treated and n-methylol melamine-modified wood of koto (pterygota macrocarpa k. schum.) and limba (terminalia superba engl. et. diels). *Holzforschung*, 67:137–146.
- [Maki et al., 1995] Maki, A., Yamashita, Y., Ito, Y., Watanabe, E., Mayanagi, Y., and Koizumi, H. (1995). Spatical and temporal analysis of human motor activity using non-invasive nir topography. *Med. Phys.*, 22:1997–2005.
- [Moghaddam et al., 2014] Moghaddam, M. S., Claesson, P. M., Walinder, M. E. P., and Swerin, A. (2014). Wettability and liquid sorption of wood investigated by wilhelmy plate method. *Wood Sci. Technol.*, 48:161–176.
- [Moore, 2011] Moore, J. (2011). Wood properties and uses of sitka spruce in britain. Technical report, Forestry Commission Research Report, Forestry Commission, Silvan House, Edinburgh, EH12 7AT.
- [Morra et al., 1991] Morra, M. J., Hall, M. H., and Freeborn, L. L. (1991). Carbon and nitrogen analysis of soil fraction using near-infra-red reflectance spectroscopy. *Soil Sci. Soc. Am. J.*, 55:288–291.
- [Muin and Tsunoda, 2004] Muin, M. and Tsunoda, K. (2004). Retention of silafluofen in wood-based composites after supercritical carbon dioxide impregnation. *Forest Prod. J.*, 54:168–171.
- [Nicolai et al., 2008] Nicolai, B. M., Verlinden, B. E., Desmet, M., Saevels, S., Saeys, W., Theron, K., Cubeddu, R., Pifferi, A., and Torricelli, A. (2008). Time-resolved and continuous wave nir reflectance spectroscopy to predict soluble solids content and firmness of pear. *Postharvest Biol. Technol.*, 47:68–74.
- [Patterson et al., 1989] Patterson, M. S., Chance, B., and Wilson, B. C. (1989). Time resolved reflectance and transmittance for the noninvasive measurement of tissue optical properties. *Appl. Optics*, 28:2331–2336.
- [Perre and Turner, 2001] Perre, P. and Turner, I. (2001). Determination of the material property variation across the growth ring of softwood for use in a heterogeneous drying model. part i - capillary pressure, tracheid model and absolute permeability. *Holz-forschung*, 55:318–323.
- [Reed and Wilson, 1993] Reed, C. M. and Wilson, N. (1993). The fundamentals of absorbency of fibres, textile structures and polymers i: the rate of rise of a liquid in glass capillaries. *J. Phys. D: Appl. Phys.*, 26:1378–1381.
- [Schultz et al., 2008] Schultz, T. P., Militz, H., Freeman, M. H., Goodell, B., and Nicholas, D. D. (2008). *Development of commercail wood preservativesL Efficacy, Environmental, and health issues*. ACS Symposium series 982. American Chemical Society, American Chemical Society, Washington, DC.
- [Siau, 1984] Siau, J. F. (1984). *Transport processes in wood*. Springer series on Wood Science. Spring-Verlag.
- [Steppe et al., 2004] Steppe, K., Cnudde, V., Girard, C., Lemeur, R., Cubeddu, J.-P., and Jacobs, P. (2004). Use of x-ray computed microtomography for non-invasive determination of wood anatomical characteristics. *J. Struct. Biol.*, 148:11–21.
- [Suzuki et al., 1999] Suzuki, S., Takasaki, S., Ozaki, T., and Kobayashi, Y. (1999). A tissue oxygenation monitor using nir spatially resolved spectroscopy. 3597:582–592.
- [Telkki et al., 2013] Telkki, V.-V., Yliniemi, M., and Jokisaari, J. (2013). Moisture in softwoods: fiber saturation point, hydroxyl site content, and the amount of micropores as determined from nmr relaxation time distributions. *Holzforschung*, 67:291–300.
- [Tsuchikawa and Schwanninger, 2013] Tsuchikawa, S. and Schwanninger, M. (2013). A review of recent near-infrared research for wood and paper (part 2). *Appl. Spectrosc. Rev.*, 48:560–587.
- [Tyree and Ewers, 1991] Tyree, M. T. and Ewers, F. W. (1991). Tansley review no. 34 - the hydraulic architecture of trees and other woody plants. *New Phytol.*, 119:345–360.
- [Villringer and Chance, 1997] Villringer, A. and Chance, B. (1997). Non-invasive optical spectroscopy and imaging of human brain function. *Trends Neurosci.*, 20:435–442.

- [Xie et al., 2011] Xie, Y., Hill, C. A. S., Jalaludin, Z., Curling, S. J., Anandjiwala, R. D., Norton, A. J., and Newman, G. (2011). The dynamic water vapour sorption behaviour of natural fibres and kinetic analysis using the parallel exponential kinetics model. *J. Mater. Sci.*, 46:479–489.
- [Yamada et al., 2006] Yamada, T., Yeh, T.-Y., Chang, H.-M., Li, L., Kadla, J. F., and Chiang, V. L. (2006). Rapid analysis of transgenic trees using transmittance near-infrared spectroscopy (nir). *Holzforschung*, 60:24–28.
- [Zhang et al., 2014] Zhang, J., Miao, P., Zhong, D., and Liu, L. (2014). Mathematical modeling of drying masson pine lumber and its asymmetrical moisture content profile. *Holzforschung*, 63:313–321.
- [Zhang et al., 2007] Zhang, Y., Wang, H., Zhang, C., and Chen, Y. (2007). Modeling of capillary flow in shaped polymer fiber bundles. *J. Mater. Sci.*, 42:8035–8039.
- [Zhang et al., 2006] Zhang, Y., Zhang, S. Y., Yang, D. Q., and Wan, H. (2006). Dimensional stability of wood-polymer composites. *J. Appl. Polym. Sci.*, 102:5085–5094.